Journal of Solution Chemistry (2020) 49:614–628
https://doi.org/10.1007/s10953-020-00973-5

Extending the Marcus μ-Scale of Solvent Softness Using Conceptual Density Functional Theory and the Orbital Overlap Distance: Method and Application to Ionic Liquids

Arshad Mehmood[1] · **Benjamin G. Janesko**[1]

Received: 27 July 2019 / Accepted: 21 January 2020 / Published online: 21 May 2020

Abstract
The chemical hardness of a solvent can play a decisive role in solubility and reactivity in solution. Several empirical scales quantifying solvent softness have been proposed. We explore whether computed properties of solvent molecules can reproduce these experimental scales. Our "orbital overlap distance" quantifying the size of orbitals at a molecule's surface effectively reproduces the Marcus μ-scale of solvent softness. The orbital overlap distance predicts that the surface of chemically hard solvent molecules is dominated by compact orbitals possessing a small orbital overlap distance. In contrast, the surface of chemically soft solvent molecules has a larger contribution from diffuse orbitals and a larger orbital overlap distance. Other conceptual density functional theory descriptors, including the global hardness and electronegativity, can also reproduce the Marcus scale. We further introduce a "solvent versatility" RMSD D_{surf} scale quantifying variations in the surface orbital overlap distance. "Good" solvents such as DMSO, which combine chemically "hard" and "soft" sites within a single molecule, possess a large RMSD D_{surf}. We conclude by applying this approach to predict the Marcus μ-parameters for widely-used ionic liquids and ionic liquid–cosolvent systems.

Keywords Computational chemistry · Ionic liquids · Molecular modeling · Density functional theory · Solvents

1 Introduction

The Lewis concept of acids as electron pair acceptors and bases as electron pair donors [1, 2] can explain certain aspects of solvation, as solvent and solute both may act as donors and/or acceptors [3]. Pearson's concept of hard and soft acids and bases (HSAB)

Electronic supplementary material The online version of this article (https://doi.org/10.1007/s10953-020-00973-5) contains supplementary material, which is available to authorized users.

✉ Arshad Mehmood
arshad.mehmood@tcu.edu

[1] Department of Chemistry and Biochemistry, Texas Christian University, 2800 S. University Drive, Fort Worth, TX 76129, USA

[4, 5] can help rationalize such donor–acceptor interactions and can be extended to solvation [3]. HSAB theory suggests that, for acids and bases of comparable strength, chemically "hard" and nonpolarizable acids prefer to interact with hard bases and vice versa. Extension of this concept to solutions implies that chemically hard solvents tend to dissolve hard solutes and soft solvents dissolve soft solutes [6, 7].

Several aspects of solution chemistry have been attributed to solvent hardness and softness. In aqueous–organic solvent mixtures, the sulfates of "soft" Cd^{2+} tend to become less soluble with increasing water content, whereas sulfates of harder 3d cations like Cu^{2+} and Co^{2+} show the opposite trend [8]. The relatively hard chloride salts of Ni^{2+} and Co^{2+} show higher solubility with increasing water content, whereas the softer bromide salts show the opposite trend [9]. Metal cation complexes of *N*-phenylaza-15-crown-5 show stability order $Ca^{2+} > Cd^{2+} > Mg^{2+} > Ag^{+}$ in soft solvent acetonitrile (Marcus $\mu = 0.35$), but the opposite order occurs in harder methanol (Marcus $\mu = 0.02$) [10]. Phenol alkylation by 3-bromopropene produces mostly allyl phenyl ether in "harder" solvent acetone (Marcus $\mu = 0.03$) and mostly *o*-allyl phenol in "softer" solvents benzene or toluene (Marcus $\mu = 0.3$–0.4), illustrating solvent effects on *O*/*C* alkylation [7, 11]. Sodium phenolate alkylation by 3-chloropropene gives near 100% *O*-alkylation in ethanol and only 22% *O*-alkylation in phenol [12, 13]. Similar solvent effects are found for nucleophilic substitution and elimination [14–16]. The Witting reaction proceeds much more rapidly in DMSO than in other solvents [17]. In DMSO, the oxygen reduction and evolution reactions of Li–air batteries follow a reversible one-electron O_2/O_2^{2-} pathway whereas the same reaction in acetonitrile or dimethyl ether yields reduction to O_2^{2-} and O^{2-} [18]. Nonlinearities in the measured Marcus μ values of water–acetonitrile mixtures quantify the degree of microscopic heterogeneity [19]. A similar solvent dependence is seen in ionic liquids (ILs) [20]. In addition, the substitutions of soft/hard groups on ILs imparts a drastic change of viscosity, enthalpy of vaporization and the ion conductivities of those ILs [21]; also, the hardness/softness of ions of ILs directly controls the solubility of materials like polymers in them [22, 23].

Several groups have proposed empirical scales of solvent softness. These are based on measured Gibbs energy of transfer of metal ions [24], infrared or Raman spectral shifts [25, 26], half-wave potentials [27], reaction enthalpies [28, 29], second-order rate constants [30], fluorescence shifts [31], and so on [32]. The donor number D_N scale of Gutmann is based on the enthalpy for solvent coordination to the soft Lewis acid antimony (V) chloride in a diluted 1,2-dichloroethane medium [33]. The D_S scale of Persson et al. [34, 35] is based on the solvent-induced shift in the position of the Raman band for Hg–Br bond symmetric stretching in $HgBr_2$. D_S values are available for a large number of solvents [3]. The B_{hard} and B_{soft} scales of solvent hard and soft basicity [26] are respectively based on infrared absorbance solvatochromic shifts of phenol O–H stretching and iodoacetylene I–C stretching. The μ-scale of solvent softness proposed by Marcus [3, 24] is based on the difference between Gibbs energies of transfer for "soft" Ag^{+} vs. "hard" Na^{+} and K^{+} ions [24].

The continued development of new solvent systems motivates extension of these solvent scales. Here we explore how electronic structure simulations enable such extensions. The connection between electronic structure and chemical hardness is well-established in the realm of conceptual density functional theory (DFT), a branch of DFT which deals with the extraction of chemically relevant concepts and principles from the computational DFT [36]. Parr and Pearson [37] defined an isolated system's global hardness as the second derivative of energy with respect to the number of electrons when the external potential is held fixed [38]:

$$\eta \equiv \left(\frac{\partial^2 E}{\partial N^2}\right)_{v(r)} \tag{1}$$

The global softness is the inverse of hardness $S = 1/\eta$ [39]. One may approximate η in terms of the computed vertical ionization potential I and electron affinity A [37]:

$$\eta \approx I - A \tag{2}$$

One may also approximate η in terms of the computed highest occupied orbital (HOMO) and lowest unoccupied orbital (LUMO) energies (supporting information Fig. S1) [36]:

$$Gap = \epsilon_{\mathrm{LUMO}} - \epsilon_{\mathrm{HOMO}} \tag{3}$$

Previous studies have demonstrated that the chemical hardness calculated from Eq. 3 provides sufficiently accurate results at the Hartree–Fock (HF) level [40–42]. Beyond HF and at DFT level, this method becomes strongly dependent on the basis set and exchange correlation potential used in DFT calculations [36, 43]. Computed absolute hardness and softness have been extensively applied in areas including organic reactivity [44–47], aromaticity [48], coordination complexes [49–51], surface chemistry [52], biological systems [53] and so on [36, 52, 54, 55]. However, systematic applications to solvent hardness and softness are scarce.

The conceptual DFT description of electronegativity and chemical hardness can struggle to distinguish the chemistry of different sites on a single molecule [36]. Electrostatic properties are often modeled in terms of the molecular electrostatic potential MESP $V(\mathbf{r})$ computed on a density isosurface [56–58]. We have developed a complementary quantity, the "orbital overlap distance" $D(\mathbf{r})$, to quantify whether the orbitals at a given point are compact or diffuse. Figure 1 illustrates evaluation of the orbital overlap distance on the surface of mercaptoethanol. The orbital overlap distance is constructed from the one-particle density matrix $\gamma(\mathbf{r},\mathbf{r}') = \Sigma_i n_i \psi_i(\mathbf{r})\psi_i(\mathbf{r}')$ of molecular orbitals ψ_i with nonzero occupancy n_i. At each point $\mathbf{r}$, we evaluate the overlap with an s-orbital-like test function $C_d \exp(-|\mathbf{r} - \mathbf{r}'|^2/d^2)$ centered at point $\mathbf{r}$ and having width d:

$$\mathrm{EDR}(\mathbf{r};d) = \rho^{-\frac{1}{2}}(\mathbf{r}) \int \mathrm{d}^3\mathbf{r}'\,\gamma\left(\mathbf{r},\mathbf{r}'\right) C_d \exp\left(-\frac{\left|\mathbf{r}-\mathbf{r}'\right|^2}{d^2}\right) \tag{4}$$

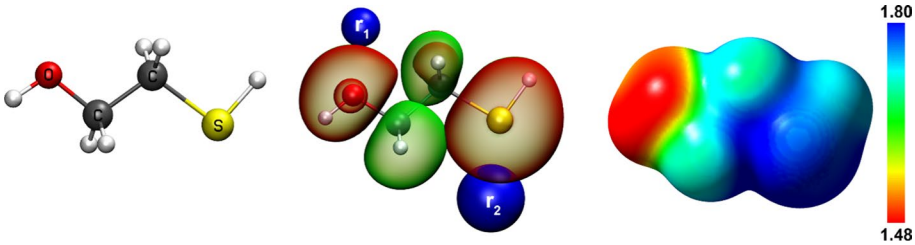

Fig. 1 The orbital overlap distance in mercaptoethanol (left) and optimized geometry (middle): evaluation of $D(\mathbf{r})$ at two points $\mathbf{r}_1$ and $\mathbf{r}_2$ near O and S lone pairs, respectively. Green and red surfaces are representative occupied orbitals HOMO and HOMO-1, plotted on the $|\psi(\mathbf{r})|^2 = 0.007$ e·Å^{-3} surface. Blue surfaces are the test function of Eq. 4, plotted at 80% of its maximum value. The test functions' overlap with all occupied MOs is maximized for widths $D(\mathbf{r}_1) = 1.5$ Å and $D(\mathbf{r}_2) = 1.8$ Å. Right: $D(\mathbf{r})$ plotted across the entire electron density isosurface on 0.007 e·Å^{-3} electron density surface (Color figure online)

The orbital overlap distance $D(\mathbf{r})$ is the distance d that maximizes this quantity at point $\mathbf{r}$. Figure 1 illustrates that compact, chemically "hard" regions (i.e. oxygen) tend to give small $D(\mathbf{r})$ values, whereas chemically "soft" regions (i.e. sulfur) tend to give larger $D(\mathbf{r})$ [59, 60]. The findings of Fig. 1 compliment the experimental results that sulfur is a good donor for soft Cu^+ and Ag^+ transition metal ions whereas oxygen is a good donor for hard alkali metal cations [61]. Plots of $D(\mathbf{r})$ on density isosurfaces, and quantitative analysis of such surfaces, complement MESP and capture trends in aromaticity, nucleophilicity, allotrope stability, and substituent effects [59, 60]. The present work applies the surface-averaged orbital overlap distance D_{surf}, as well as computed global softness, to model empirical solvent softness scales.

A key result of this work is the extension of the Marcus μ-scale to ionic liquid (IL) solvents. ILs, composed of organic cation and anion combinations have led to applications including capacitors, fuel-cell, batteries, lubricants, dye-sensitized solar cells and sensor technologies [62–66]. Cosolvents such as H_2O or DMSO can lower the IL's viscosity and improve their performance [67]. The hard/soft nature of IL counter ions and cosolvents [20–23] motivates quantitative characterization of their chemical softness/hardness.

2 Computational Details

The μ values of solvents used in the present study were taken from Ref. [24]. All calculations were performed with the Gaussian 09 [68] suite of programs. All calculations were carried out in gas-phase using the three parameter hybrid exchange functional developed by Becke [69] in conjunction with the exchange–correlation potential, corrected via a gradient developed by Lee et al. (B3LYP) [70]. All calculations used the 6-31+g(d,p) basis set [71–75], however supporting information Table S4 compares the results obtained using different basis sets. For all systems, the values of $D(\mathbf{r})$, the HOMO–LUMO energy gap and the global softness were calculated at geometries optimized to their global minimum using tight convergence criteria. For the calculation of global softness, vertical ionization potentials and electron affinities were used. Quantitative analysis of $D(\mathbf{r})$ on 0.007 e Å^{-3} electron density molecular surfaces were performed using a modified version of Multiwfn V3.6 (dev) [76, 77] to get the mean D_{surf} and RMSD D_{surf} values.

3 Results and Discussion

3.1 Correlation of Measured Marcus μ with Computed D_{surf} and Global Softness

We begin by correlating the solvent molecules' computed surface-averaged orbital overlap distance, global softness, and HOMO–LUMO gap to their measured empirical Marcus μ-scale values. We first consider the 34 solvents in Table I of Ref. [24]. Figure 2 plots the solvents' μ values vs. the computed surface-averaged overlap distance D_{surf} or global softness $1/\eta$ (Eq. 2). Table 1 reports linear fits of μ to these data. Additionally, Fig. S1 shows the HOMO and LUMO orbitals of representative solvent molecules and Fig. S2 shows the corresponding plot of μ vs. $1/Gap$, with trends matching $1/\eta$. Table S1 of the supporting information lists all computed values. Figure S3 shows the relation between D_{surf} and $1/Gap$.

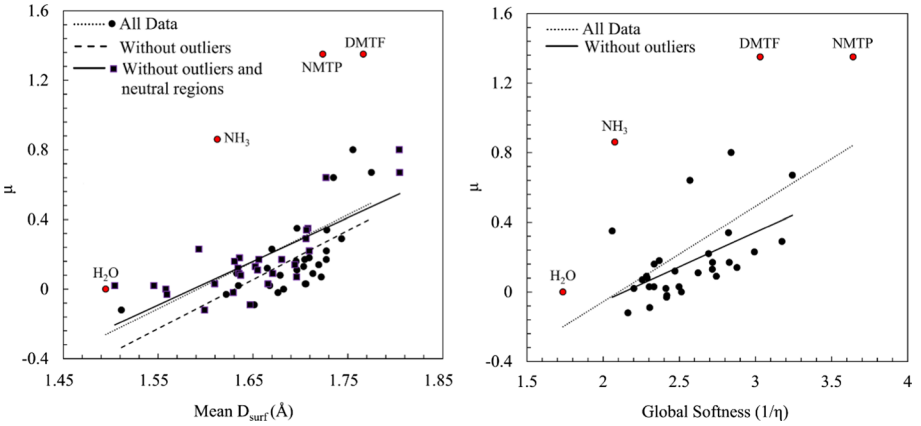

Fig. 2 Measured Marcus μ parameters (ordinate) plotted vs. computed D_{surf} (left) or computed global softness $1/\eta$ (Eq. 2). Results for the 34 solvents in Table 1 of Ref. [24]. Important outliers are highlighted

Table 1 Linear fits of the experimental Marcus μ parameter to computed D_{surf}, global softness $1/\eta$ (Eq. 2), or HOMO–LUMO Gap (Eq. 3)

Method	Data	Equation	R^2	MAE	ME	RMSD
D_{surf}	A	$\mu = 1.349\ D_{surf} - 4.026$ (4)	0.209	0.230	0.000	0.321
	B	$\mu = 1.413\ D_{surf} - 4.325$ (5)	0.445	0.126	0.000	0.159
	C	$\mu = 1.418\ D_{surf} - 4.249$ (6)	0.659	0.244	– 0.147	0.804
$1/\eta$	A	$\mu = 0.397(1/\eta) - 0.848$ (7)	0.292	0.194	– 0.082	0.312
	B	$\mu = 0.547(1/\eta) - 1.150$ (8)	0.331	0.170	0.082	0.203
$1/Gap$	A	$\mu = 0.277(1/G) - 0.891$ (9)	0.531	0.176	0.000	0.247
	B	$\mu = 0.214(1/G) - 0.687$ (10)	0.294	0.123	0.000	0.180

Fits are performed for the 34 solvents in Table I of Ref. [24]

A all data, *B* without outliers, *C* without outliers, D_{surf} on charged areas only, *MAE* mean absolute error, *ME* mean error, *RMSD* root-mean-square deviation

Figure 2 shows a broadly consistent relation between computed and experimental values: solvents that are "soft" by the Marcus scale have large computed surface overlap distance D_{surf} and large computed global softness $1/\eta$. Chemically, the "softness" measured by the Marcus μ-scale is broadly consistent with "softness" as envisioned by conceptual DFT. Moreover, this softness is an intrinsic property of the molecules in question, such that the global softness $1/\eta$ computed for an *isolated* solvent molecule is broadly predictive of its Marcus μ in a condensed phase.

Additional chemical insight comes from the four outliers in Fig. 2: ammonia, water, *N*-methylthiopyrrolidinone (NMTP), and *N*,*N*-dimethylthioformamide (DMTF). These are by the Marcus scale softer than expected given their global hardness and D_{surf} values. These outliers are not the result of an "error" in the computed values, rather they are an important indication of these specific solvents' "special" coordination chemistry i.e. Ag^+, Na^+ and K^+ may undergo coordination with these solvents in addition to dissolution. Sandstrom and coworkers [35] found that ammonia, NMTP, DMTF, and water were major outliers in an otherwise reasonably linear relation between the μ and D_S

scales. These are visible as labeled points 70, 73, and 76 in Ref. [35], Fig. 6c. These authors rationalized the results for water in terms of its coordination to the Marcus probe ions. Experimentally, aqueous solutions of Ag^+ show four loosely coordinated water molecules, whereas aqueous solutions of Na^+ and K^+ show higher coordination numbers [35, 78]. While those authors did not explain the chemistry behind the other outliers, the fact that our calculations reproduce the "special" experimental behavior of these solvents is encouraging. Omitting these four outliers significantly improves the correlation between measured and computed values. The best fit to μ comes from averaging the orbital overlap distance over charged regions of the molecule surface, i.e., those points $\mathbf{r}$ on the surface possessing molecular electrostatic potential $|V(\mathbf{r})| > 0.04$ a.u. This technique reduces contributions from neutral alkyl chains, which are likely not much involved in the differential coordination of Ag^+ vs. Na^+ and K^+.

We next consider the estimated Marcus μ-values of 60 additional solvents, reported in Table 2 of Ref. [24], and evaluate them from either a linear fit to D_S or the difference between the B_{hard} and B_{soft} measures of hard and soft basicity. Figure 3 plots μ vs. the computed surface-averaged orbital overlap distance D_{surf}. Cases where the two spectroscopic measures of μ "grossly disagree" are plotted as asterisks. Figure 3 provides additional insight into the chemistry of the relation between orbital overlap distance and Marcus's μ. Solvents with large experimental μ values invariably possess large D_{surf}. For example, every solvent with $D_{surf} < 1.69$ Å has $\mu < 0.3$, and every solvent with $D_{surf} < 1.73$ Å has $\mu < 0.8$. Supporting Information Fig. S4 shows that this trend does not hold as well for global softness $1/Gap$, which proves to be somewhat worse than D_{surf} at predicting these μ values.

Chemically, solvents with small experimental μ values tend to have smaller D_{surf}, consistent with compact regions of small orbital overlap distance. Solvents that combine a small Marcus μ with a large D_{surf} tend to be weakly coordinating. For example, benzene, tetrahydrofuran, acetonitrile, and benzonitrile have one of the two spectroscopic measures assign $\mu < 0$, and all have relatively large $D_{surf} > 1.69$ Å.

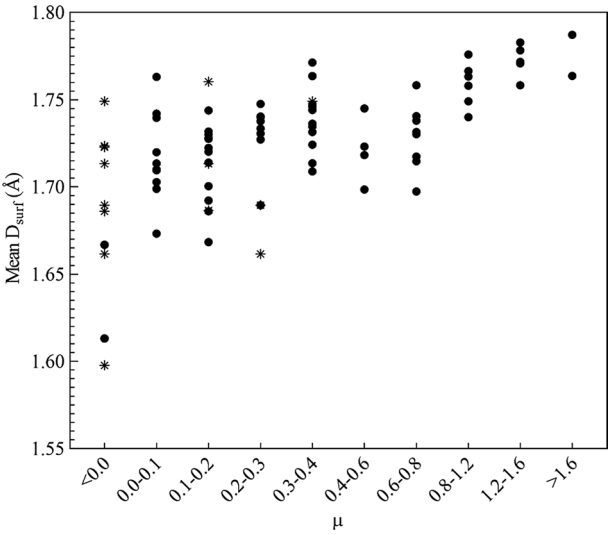

Fig. 3 Correlation between Marcus's μ-scale and mean D_{surf} of solvents mentioned in Table 2 of Ref. [24]. Asterisks show those data points where the two spectroscopic measures of μ "grossly disagree"

3.2 Extension to Other Empirical Solvent Scales

We next consider whether the computed electronegativity and global softness, or computed D_{surf} and surface-averaged electrostatic potential V_{surf}, can be predictive for other solvent scales. Table 2 shows fits of the empirical μ, D_S, and *DN* scales. Fits are to 26 different solvents for which μ, D_S, and *DN* are well-known (Ref [35]). All computed and experimental values are in the supplementary information Table S2. The results in Table 2 are again instructive. The combination of D_{surf} and V_{surf} does a better job of modeling the Marcus μ scale, giving a RMSD lower than the corresponding fit to electronegativity and global softness. In contrast, electronegativity and global softness give somewhat smaller RMSD values for the D_S and *DN* scales. Hardness and orbital-overlap descriptors are relatively more important for modeling the μ scale. Considering first the fits to V_{surf} and D_{surf}, the best-fit coefficient of V_{surf} is 40–150 times that of D_{surf} for the D_S and *DN* scales, but only four times that of D_{surf} for the μ scale. Similarly, for the fits to electronegativity and global softness, the best-fit coefficient of electronegativity is 20–2800 times that of global softness for D_S and *DN* scales, but only two times that of global softness for the μ scale. This is consistent with the suggestion that D_S and *DN* quantify a solvent's "soft donor ability", i.e. these scales are based on the soft acceptor molecules $HgBr_2$ and $SbCl_5$ respectively [35], whereas μ quantifies a solvent's relative soft vs. hard donation.

3.3 Variations in Surface Overlap Distance

Figure 1 shows how the orbital overlap distance effectively differentiates regions of a molecule surface dominated by compact vs. diffuse orbitals. Accordingly, variations in the orbital overlap distance across a surface (RMSD D_{surf}) should provide information about the variety of solvating interactions available. Figure 4 plots the mean D_{surf} vs. RMSD D_{surf} values of 34 solvents in Table I of Ref. [24].

Molecules which have both hard and soft regions on their molecular surface exhibit large value of RMSD D_{surf}. Table S1 shows the calculated RMSD D_{surf} for a number of solvents. Solvents like mercaptoethanol, DMSO and *N*-methylformamide have large value of RMSD D_{surf}, which compliments their ability to dissolve a variety of hard or soft substances. Similarly, 2,2,2-trifluoroethanol, propylene carbonate and 1,2-ethanediol also show large values of RMSD D_{surf} which explains their versatile solvating ability. Solvents like water, ammonia, tetrahydrothiophene, acetonitrile and 1,1-dichloroethane have relatively small values of RMSD D_{surf} which is in accordance to their ability to dissolve only limited substances of specific hard/soft nature. Water, having a hard oxygen atom with little variations on D_{surf}, have small value of RMSD D_{surf}, whereas alcohols have higher value

Table 2 Linear fits of experimental μ, *D*s and *DN* solvent scales to computed D_{surf}, V_{surf} and global softness $1/\eta$ and electronegativity χ of 26 different solvents

Formula	RMSD	HS
$\mu = 1.95\ D_{surf} - 7.17\ V_{surf} - 6.02$	0.622	4
$D_S = 65.0\ D_{surf} - 2651\ V_{surf} - 177$	0.276	40
$DN = 21.5\ D_{surf} - 3328\ V_{surf} - 33$	0.417	154
$\mu = 0.26/\eta - 0.48\ \chi - 0.41$	0.707	2
$D_S = -0.11/\eta - 313\ \chi + 71.9$	0.245	2800
$DN = -15.3/\eta - 413\ \chi + 130$	0.366	27

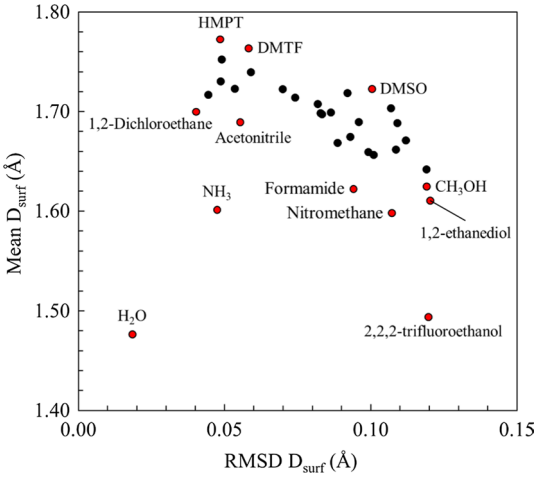

Fig. 4 Correlation between mean D_{surf} and RMSD D_{surf} of solvents mentioned in Table 1 of Ref. [24] elaborating the versatility of solvents. The outliers are highlighted using red filled circles (Color figure online)

compared to water and RMSD D_{surf} increases with increase in the number of carbon atoms. Both acetone and 1,2-dichloroethane have the same value of μ and nearly equal values of mean D_{surf}, but the large RMSD D_{surf} of the former compound explains its large dissolving ability compared to other one.

3.4 Applications to Ionic Liquids

We used the obtained best linear fitting model (Eq. 6 of Table 1) to predict the μ values for selected 20 ionic liquids (ILs). Table S3 (SI) lists the full names of these ILs. Table 3 shows the predicted values along with mean D_{surf} and RMSD D_{surf} values of each ionic liquid system. The table indicates that the anionic part plays a fundamental role in controlling the softness of the ionic liquid. Ionic liquids having [Br] and [Cl] as anions have large values of μ, indicating their chemical softness, whereas those ILs which combine hard anions [CF_3SO_3] and [PF_6] have small μ values owing to their chemical hardness. Similarly, ILs with the [$MeSO_4$] anion shows intermediate value of μ. For the same anion, the cations [$N_{1\,1\,1\,6}$] and [C_2py] impart large μ values to ionic liquids compared to the [emim] and [mPhim] cations. Table 3 shows that RMSD D_{surf} increases with decrease in mean D_{surf} value where ionic liquids having hard anions and small μ values show large RMSD D_{surf}. This shows that hard ILs have large solvating abilities.

Both theory and experiments suggest that ions of ILs can exist in multiple conformations [79, 80]. To quantify the variations in mean D_{surf} and RMSD D_{surf} values due to different conformations, we calculated these quantities for two conformations, *trans–trans* (TT) and *gauche-trans* (GT) of 1-butyl-3-methylimidazolium [81], as an illustration. Figure 5 shows that mean D_{surf} is same for both conformations, which suggests that conformational changes do not have a profound effect on the chemical softness of ILs. Similarly, RMSD D_{surf} also shows insignificant variation with conformational changes, which establishes that the solvating ability is not significantly affected by conformational equilibria. It can be inferred from these results that the reported method to estimate μ is equally valid for all the adopted conformations of solvent molecules and the optimized geometry of a single conformation gives a reliable estimate of μ for all other conformations.

Table 3 Predicted μ values for selected ionic liquids. Full names of ILs are provided in the supporting information

Ionic liquid	Mean D_{surf} (Å)	RMSD D_{surf} (Å)	Predicted μ
$[N_{1\,1\,1\,6}][Br]$	1.785	0.065	0.536
$[C_2py][Br]$	1.773	0.083	0.503
$[N_{1\,1\,1\,6}][Cl]$	1.766	0.044	0.486
[emim][Br]	1.766	0.094	0.484
[mPhim][Br]	1.763	0.089	0.478
$[C_2py][Cl]$	1.748	0.056	0.436
[mPhim][Cl]	1.742	0.067	0.421
[emim][Cl]	1.741	0.070	0.419
$[N_{1\,1\,1\,6}][MeSO_4]$	1.705	0.094	0.321
$[mPhim][MeSO_4]$	1.680	0.093	0.255
$[C_2py][MeSO_4]$	1.674	0.090	0.239
$[emim][MeSO_4]$	1.671	0.094	0.230
$[N_{1\,1\,1\,6}][CF_3SO_3]$	1.663	0.133	0.209
$[N_{1\,1\,1\,6}][PF_6]$	1.647	0.159	0.166
$[mPhim][CF_3SO_3]$	1.636	0.126	0.137
$[C_2py][CF_3SO_3]$	1.623	0.125	0.101
$[emim][CF_3SO_3]$	1.621	0.126	0.096
$[mPhim][PF_6]$	1.617	0.151	0.086
$[C_2py][PF_6]$	1.599	0.152	0.038
$[emim][PF_6]$	1.598	0.152	0.034

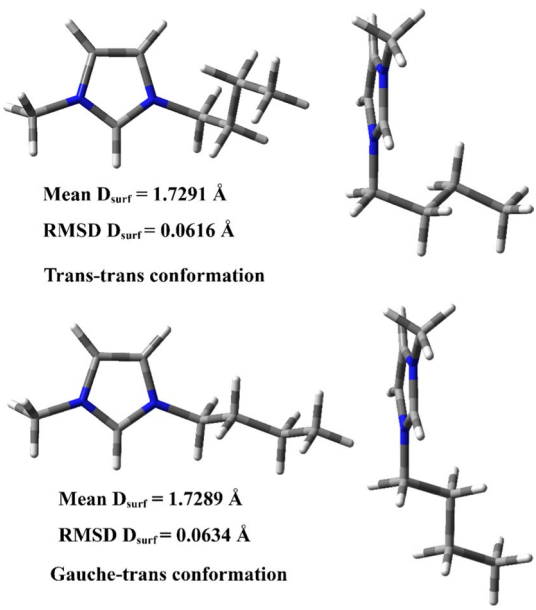

Fig. 5 Optimized geometries and claculated mean D_{surf} and RMSD D_{surf} of two 1-butyl-3-methylimidazolium conformations

Table 4 Predicted μ values for selected ionic liquids and ionic liquids/cosolvents along with mean and RMSD D_{surf}

Ionic liquid	Without cosolvent			Water as cosolvent			DMSO as cosolvent		
	Mean D_{surf} (Å)	RMSD D_{surf} (Å)	Predicted μ	Mean D_{surf} (Å)	RMSD D_{surf} (Å)	Predicted μ	Mean D_{surf} (Å)	RMSD D_{surf} (Å)	Predicted μ
$[P_{4\,4\,4\,4}][Ac]$	1.738	0.065	0.409	1.715	0.096	0.349	1.735	0.073	0.401
$[P_{4\,4\,4\,4}][DCA]$	1.735	0.064	0.402	1.713	0.095	0.343	1.733	0.073	0.396
$[C_8mim][Ac]$	1.725	0.078	0.376	1.700	0.106	0.307	1.725	0.083	0.374
$[C_8mim][DCA]$	1.722	0.076	0.368	1.697	0.104	0.300	1.722	0.082	0.368
[bpy][Ac]	1.714	0.072	0.345	1.683	0.105	0.262	1.716	0.081	0.352
$[P_{4\,4\,4\,4}][NO_3]$	1.713	0.098	0.343	1.692	0.116	0.286	1.715	0.099	0.348
$[C_4mim][Ac]$	1.710	0.079	0.335	1.680	0.107	0.255	1.713	0.085	0.344
[bpy][DCA]	1.710	0.070	0.335	1.680	0.102	0.255	1.713	0.080	0.344
$[C_4mim][DCA]$	1.706	0.076	0.325	1.677	0.105	0.248	1.711	0.084	0.337
$[C_8mim][NO_3]$	1.694	0.109	0.292	1.671	0.123	0.229	1.701	0.108	0.310
$[P_{4\,4\,4\,4}][BF_4]$	1.692	0.133	0.287	1.673	0.141	0.236	1.698	0.128	0.303
$[N_{1\,1\,1\,2OH}][Ac]$	1.690	0.100	0.280	1.657	0.120	0.194	1.700	0.101	0.308
$[N_{1\,1\,1\,2OH}][DCA]$	1.686	0.097	0.270	1.655	0.116	0.188	1.697	0.099	0.300
$[bpy][NO_3]$	1.672	0.107	0.233	1.645	0.120	0.160	1.687	0.108	0.272
$[C_8mim][BF_4]$	1.669	0.144	0.225	1.648	0.149	0.170	1.681	0.137	0.258
$[C_4mim][NO_3]$	1.669	0.110	0.225	1.643	0.122	0.155	1.684	0.110	0.266
$[P_{4\,4\,4\,4}][NTf_2]$	1.661	0.139	0.203	1.648	0.143	0.168	1.671	0.136	0.230
$[bpy][BF_4]$	1.639	0.146	0.145	1.617	0.147	0.086	1.663	0.140	0.209
$[N_{1\,1\,1\,2OH}][NO_3]$	1.638	0.122	0.142	1.612	0.126	0.073	1.666	0.122	0.216
$[C_8mim][NTf_2]$	1.637	0.143	0.140	1.624	0.144	0.104	1.654	0.140	0.184
$[C_4mim][BF_4]$	1.637	0.147	0.140	1.616	0.148	0.083	1.661	0.141	0.204
$[bpy][NTf_2]$	1.609	0.139	0.064	1.596	0.138	0.029	1.634	0.139	0.132
$[C_4mim][NTf_2]$	1.608	0.139	0.062	1.595	0.138	0.027	1.633	0.140	0.129
$[N_{1\,1\,1\,2OH}][BF_4]$	1.600	0.154	0.041	1.581	0.149	− 0.011	1.640	0.150	0.146
$[N_{1\,1\,1\,2OH}][NTf_2]$	1.579	0.138	− 0.016	1.568	0.134	− 0.047	1.614	0.144	0.077

Full names of ILs are provided in the Supporting Information

We end by predicting the μ values for binary ILs/cosolvents systems by considering water and DMSO as cosolvents for 25 ionic liquids systems. Table 4 presents the calculated μ values for pure ILs, ILs/water and ILs/DMSO binary systems. For all ILs, the addition of water results a decrease in the μ values and for ILs $[N_{1\,1\,1\,2}OH][BF_4]$ and $[N_{1\,1\,1\,2}OH][NTf_2]$ it becomes negative. Whereas, the addition of DMSO results an increase in the μ values for most of ILs. In some cases, the addition of DMSO as cosolvent imparts insignificant variations to the predicted μ values which can be attributed to the combined mean D_{surf} of IL components being comparable to that of DMSO. These results compliment the experimental findings about dissolution of cellulose in some ILs, which demonstrate that the addition of DMSO to ILs/cellulose system enhances the solubility of cellulose, whereas the addition of water or ethanol precipitate cellulose from these systems [82–84].

4 Conclusions

Our orbital overlap distance $D(\mathbf{r})$ distinguishes the chemically hard and soft regions on the surface of a molecule; hence we related the mean D_{surf} value to the chemical softness/hardness of solvent molecules. We proposed a method to estimate the Marcus's μ values of solvent softness by fitting μ with the calculated mean D_{surf}. We showed that both the mean D_{surf} and global softness provide reasonable estimate of solvent softness. The surface variation of $D(\mathbf{r})$, i.e. RMSD D_{surf}, is related to the solvation ability of solvent where large RMSD D_{surf} values show that the solvent can dissolve both hard and soft solutes. We reported the extension to some other scales of "solvent soft basicity". We used the proposed method to predict Marcus μ values for ILs and IL/cosolvent systems.

Acknowledgements This work was supported by the National Science Foundation (DMR-1505343).

References

1. Lewis, G.N.: Valence and the Structure of Atoms and Molecules. Dover Publications, New York (1923)
2. Lewis, G.N.: Acids and bases. J. Franklin Inst. **226**(3), 293–313 (1938). https://doi.org/10.1016/S0016-0032(38)91691-6
3. Chen, T., Hefter, G., Marcus, Y.: Relationships among solvent softness scales. J. Solution Chem. **29**(3), 201–216 (2000). https://doi.org/10.1023/a:1005114615767
4. Pearson, R.G.: Hard and soft acids and bases. J. Am. Chem. Soc. **85**(22), 3533–3539 (1963). https://doi.org/10.1021/ja00905a001
5. Pearson, R.G.: Acids and bases. Science **151**(3707), 172–177 (1966). https://doi.org/10.1126/science.151.3707.172
6. Pearson, R.G.: Hard and soft acids and bases—the evolution of a chemical concept. Coord. Chem. Rev. **100**, 403–425 (1990). https://doi.org/10.1016/0010-8545(90)85016-L
7. Reichardt, C., Welton, T.: Solvents and Solvent Effects in Organic Chemistry. Wiley, Hoboken (2011)
8. Bogachev, N.A., Gorbunov, A.O., Tikhomirova, A.A., Pushikhina, O.S., Skripkin, M.Y., Nikolskii, A.B.: Solubility of d-elements salts in organic and aqueous-organic solvents: I. Copper, cobalt, and cadmium sulfates. Russ. J. Gen. Chem. **85**(11), 2509–2512 (2015). https://doi.org/10.1134/s107036321511002x
9. Gorbunov, A.O., Tsyrulnikov, N.A., Tikhomirova, A.A., Bogachev, N.A., Skripkin, M.Y., Nikolskii, A.B., Pestova, O.N.: Solubility of d-element salts in organic and aqueous–organic solvents: II. Effect of halocomplex formation on solubility of cobalt bromide and chloride and nickel chloride. Russ. J. Gen. Chem. **86**(4), 771–777 (2016). https://doi.org/10.1134/s1070363216040022
10. Payehghadr, M., Hashemi, S.E.: Solvent effect on complexation reactions. J. Incl. Phenom. Macrocycl. Chem. **89**(3), 253–271 (2017). https://doi.org/10.1007/s10847-017-0759-8

11. Claisen, L.: Über C-alkylierung (Kernalkylierung) von Phenolen. Angew. Chem. **36**(65), 478–479 (1923). https://doi.org/10.1002/ange.19230366502
12. Kornblum, N., Berrigan, P.J., le Noble, W.J.: Chemical effects arising from selective solvation: selective solvation as a factor in the alkylation of ambident anions. J. Am. Chem. Soc. **82**(5), 1257–1258 (1960). https://doi.org/10.1021/ja01490a063
13. Kornblum, N., Berrigan, P.J., Le Noble, W.J.: Solvation as a factor in the alkylation of ambident anions: the importance of the hydrogen bonding capacity of the solvent. J. Am. Chem. Soc. **85**(8), 1141–1147 (1963). https://doi.org/10.1021/ja00891a024
14. Hughes, E.D., Ingold, C.K.: Mechanism of substitution at a saturated carbon atom. Part IV. A discussion of constitutional and solvent effects on the mechanism, kinetics, velocity, and orientation of substitution. J. Chem. Soc. (1935). https://doi.org/10.1039/JR9350000244
15. Hughes, E.D.: Mechanism and kinetics of substitution at a saturated carbon atom. Trans. Faraday Soc. **37**, 603–631 (1941). https://doi.org/10.1039/TF9413700603
16. Cooper, K.A., Dhar, M.L., Hughes, E.D., Ingold, C.K., MacNulty, B.J., Woolf, L.I.: Mechanism of elimination reactions. Part VII. Solvent effects on rates and product-proportions in uni- and bi-molecular substitution and elimination reactions of alkyl halides and sulphonium salts in hydroxylic solvents. J. Chem. Soc. (1948). https://doi.org/10.1039/JR9480002043
17. Greenwald, R., Chaykovsky, M., Corey, E.J.: The Wittig reaction using methylsulfinyl carbanion-dimethyl sulfoxide 1. J. Org. Chem. **28**(4), 1128–1129 (1963). https://doi.org/10.1021/jo01039a502
18. Laoire, C.O., Mukerjee, S., Abraham, K.M., Plichta, E.J., Hendrickson, M.A.: Influence of nonaqueous solvents on the electrochemistry of oxygen in the rechargeable lithium−air battery. J. Phys. Chem. C **114**(19), 9178–9186 (2010). https://doi.org/10.1021/jp102019y
19. Marcus, Y.: The use of chemical probes for the characterization of solvent mixtures. Part 2. Aqueous mixtures. J. Chem. Soc. Perkin Trans. **2**(8), 1751–1758 (1994). https://doi.org/10.1039/P29940001751
20. Allen, C.J., Hwang, J., Kautz, R., Mukerjee, S., Plichta, E.J., Hendrickson, M.A., Abraham, K.M.: Oxygen reduction reactions in ionic liquids and the formulation of a general ORR mechanism for Li–air batteries. J. Phys. Chem. C **116**(39), 20755–20764 (2012). https://doi.org/10.1021/jp306718v
21. Peppel, T., Köckerling, M., Geppert-Rybczyńska, M., Ralys, R.V., Lehmann, J.K., Verevkin, S.P., Heintz, A.: Low-viscosity paramagnetic ionic liquids with doubly charged $[Co(NCS)_4]^{2-}$ Ions. Angew. Chem. Int. Ed. **49**(39), 7116–7119 (2010). https://doi.org/10.1002/anie.201000709
22. Tsurumaki, A., Trequattrini, F., Palumbo, O., Panero, S., Paolone, A., Navarra, M.A.: The effect of ether-functionalisation in ionic liquids analysed by DFT calculation, infrared spectra, and Kamlet-Taft parameters. PCCP **20**(12), 7989–7997 (2018). https://doi.org/10.1039/C7CP08134K
23. Tsurumaki, A., Kagimoto, J., Ohno, H.: Properties of polymer electrolytes composed of poly(ethylene oxide) and ionic liquids according to hard and soft acids and bases theory. Polym. Adv. Technol. **22**(8), 1223–1228 (2011). https://doi.org/10.1002/pat.1931
24. Marcus, Y.: Linear solvation energy relationships: a scale describing the "softness" of solvents. J. Phys. Chem. **91**(16), 4422–4428 (1987). https://doi.org/10.1021/j100300a044
25. Persson, I., Sandström, M., Goggin, P.L.: On the coordinating properties of some solvents. A vibrational spectroscopic study of mercury(II) halides and antimony(V) chloride in solution; new concepts for Lewis basicity scales of solvents. Inorg. Chim. Acta **129**(2), 183–197 (1987). https://doi.org/10.1016/S0020-1693(00)86662-1
26. Laurence, C., Queignec-Cabanetos, M., Dziembowska, T., Queignec, R., Wojtkowiak, B.: 1-Iodoacetylenes 1 Spectroscopic evidence of their complexes with Lewis bases. A spectroscopic scale of soft basicity. J. Am. Chem. Soc. **103**(10), 2567–2573 (1981). https://doi.org/10.1021/ja00400a014
27. Gritzner, G.: Solvent effects on half-wave potentials. J. Phys. Chem. **90**(21), 5478–5485 (1986). https://doi.org/10.1021/j100412a116
28. Gutmann, V., Wychera, E.: Coordination reactions in non aqueous solutions: the role of the donor strength. Inorg. Nucl. Chem. Lett. **2**(9), 257–260 (1966). https://doi.org/10.1016/0020-1650(66)80056-9
29. Maria, P.C., Gal, J.F.: A Lewis basicity scale for nonprotogenic solvents: enthalpies of complex formation with boron trifluoride in dichloromethane. J. Phys. Chem. **89**(7), 1296–1304 (1985). https://doi.org/10.1021/j100253a048
30. Oshima, T., Arikata, S., Nagai, T.: Solvent effects in the reaction of diazodiphenylmethane with tetracycanoethylene: a new empirical parameter of solvent basicity. J. Chem. Res. **2**, 204–205 (1981)
31. Dong, D.C., Winnik, M.A.: The Py scale of solvent polarities. Solvent effects on the vibronic fine structure of pyrene fluorescence and empirical correlations with Et and Y values. Photochem. Photobiol. **35**(1), 17–21 (1982). https://doi.org/10.1111/j.1751-1097.1982.tb03805.x
32. Katritzky, A.R., Tamm, T., Wang, Y., Sild, S., Karelson, M.: QSPR treatment of solvent scales. J. Chem. Inf. Comput. Sci. **39**(4), 684–691 (1999). https://doi.org/10.1021/ci980225h

33. Gutmann, V.: Empirical parameters for donor and acceptor properties of solvents. Electrochim. Acta **21**(9), 661–670 (1976). https://doi.org/10.1016/0013-4686(76)85034-7
34. Persson, I.: Solvation and complex formation in strongly solvating solvents. Pure Appl. Chem. **58**(8), 1153–1161 (1986)
35. Sandström, M., Persson, I., Persson, P.: A study of solvent electron-pair donor ability and Lewis basicity scales. Acta Chem. Scand **44**(7), 653–675 (1990). https://doi.org/10.3891/acta.chem.scand.44-0653
36. Geerlings, P., De Proft, F., Langenaeker, W.: Conceptual density functional theory. Chem. Rev. **103**(5), 1793–1874 (2003). https://doi.org/10.1021/cr990029p
37. Parr, R.G., Pearson, R.G.: Absolute hardness: companion parameter to absolute electronegativity. J. Am. Chem. Soc. **105**(26), 7512–7516 (1983). https://doi.org/10.1021/ja00364a005
38. Ayers, P.W.: An elementary derivation of the hard/soft-acid/base principle. J. Chem. Phys. **122**(14), 141102 (2005). https://doi.org/10.1063/1.1897374
39. Yang, W., Parr, R.G.: Hardness, softness, and the fukui function in the electronic theory of metals and catalysis. Proc. Natl. Acad. Sci. U.S.A. **82**(20), 6723–6726 (1985). https://doi.org/10.1073/pnas.82.20.6723
40. Jayakumar, N., Kolandaivel, P.: Studies of isomer stability using the maximum hardness principle (MHP). Int. J. Quantum Chem. **76**(5), 648–655 (2000). https://doi.org/10.1002/(SICI)1097-461X(2000)76:5%3c648:AID-QUA7%3e3.0.CO;2-Y
41. Padmanabhan, J., Parthasarathi, R., Subramanian, V., Chattaraj, P.K.: Molecular structure, reactivity, and toxicity of the complete series of chlorinated benzenes. J. Phys. Chem. A **109**(48), 11043–11049 (2005). https://doi.org/10.1021/jp0538621
42. Senthilkumar, K., Kolandaivel, P.: Hartree–Fock and density functional theory studies on ionization and fragmentation of halomethane molecules by positron impact. Mol. Phys. **100**(24), 3817–3822 (2002). https://doi.org/10.1080/00268970210161939
43. Shankar, R., Senthilkumar, K., Kolandaivel, P.: Calculation of ionization potential and chemical hardness: a comparative study of different methods. Int. J. Quantum Chem. **109**(4), 764–771 (2009). https://doi.org/10.1002/qua.21883
44. Geerlings, P., De Proft, F.: HSAB principle: applications of its global and local forms in organic chemistry. Int. J. Quantum Chem. **80**(2), 227–235 (2000). https://doi.org/10.1002/1097-461X(2000)80:2%3c227:AID-QUA17%3e3.0.CO;2-N
45. Langenaeker, W., de Proft, F., Geerlings, P.: Development of local hardness-related reactivity indices: their application in a study of the SE at monosubstituted benzenes within the HSAB context. J. Phys. Chem. **99**(17), 6424–6431 (1995). https://doi.org/10.1021/j100017a022
46. Mendez, F., Garcia-Garibay, M.A.: A Hard−soft acid−base and DFT analysis of singlet−triplet gaps and the addition of singlet carbenes to alkenes. J. Org. Chem. **64**(19), 7061–7066 (1999). https://doi.org/10.1021/jo990584r
47. Chattaraj, P.K., Fuentealba, P., Gómez, B., Contreras, R.: Woodward−Hoffmann rule in the light of the principles of maximum hardness and minimum polarizability: DFT and *ab initio* SCF studies. J. Am. Chem. Soc. **122**(2), 348–351 (2000). https://doi.org/10.1021/ja992337a
48. Balawender, R., Komorowski, L., De Proft, F., Geerlings, P.: Derivatives of molecular valence as a measure of aromaticity. J. Phys. Chem. A **102**(48), 9912–9917 (1998). https://doi.org/10.1021/jp982447o
49. Sarmah, P., Deka, R.C.: Solvent effect on the reactivity of CIS-platinum(II) complexes: a density functional approach. Int. J. Quantum Chem. **108**(8), 1400–1409 (2008). https://doi.org/10.1002/qua.21635
50. Panina, N.S., Calligaris, M.: Density functional study of linkage isomerism in dimethyl sulfoxide Ru(III) and Rh(III) complexes. Inorg. Chim. Acta **334**, 165–171 (2002). https://doi.org/10.1016/S0020-1693(02)00752-1
51. Bania, K.K., Deka, R.C.: Influence of Zeolite framework on the structure, properties, and reactivity of cobalt phenanthroline complex: a combined experimental and computational study. J. Phys. Chem. C **115**(19), 9601–9607 (2011). https://doi.org/10.1021/jp2003672
52. Islam, N., Kaya, S.: Conceptual Density Functional Theory and Its Application in the Chemical Domain. Apple Academic Press, New York (2018)
53. Frau, J., Hernández-Haro, N., Glossman-Mitnik, D.: Computational prediction of the pK_as of small peptides through conceptual DFT descriptors. Chem. Phys. Lett. **671**, 138–141 (2017). https://doi.org/10.1016/j.cplett.2017.01.038
54. Putz, M.V., Mingos, D.M.P.: Applications of Density Functional Theory to Chemical Reactivity. Springer, Berlin (2013)
55. Pearson, R.G.: Chemical Hardness: Applications from Molecules to Solids. Wiley, Hoboken (1998)
56. Bader, R.F.W., Carroll, M.T., Cheeseman, J.R., Chang, C.: Properties of atoms in molecules: atomic volumes. J. Am. Chem. Soc. **109**(26), 7968–7979 (1987). https://doi.org/10.1021/ja00260a006

57. Politzer, P., Murray, J.S.: σ-holes and π-holes: Similarities and differences. J. Comput. Chem. **39**(9), 464–471 (2018). https://doi.org/10.1002/jcc.24891
58. Kolář, M.H., Hobza, P.: Computer modeling of halogen bonds and other σ-hole interactions. Chem. Rev. **116**(9), 5155–5187 (2016). https://doi.org/10.1021/acs.chemrev.5b00560
59. Mehmood, A., Janesko, B.G.: An orbital-overlap complement to atomic partial charge. Angew. Chem. Int. Ed. **56**(24), 6878–6881 (2017). https://doi.org/10.1002/anie.201702715
60. Janesko, B.G., Wiberg, K.B., Scalmani, G., Frisch, M.J.: Electron delocalization range in atoms and on molecular surfaces. J. Chem. Theory Comput. **12**(7), 3185–3194 (2016). https://doi.org/10.1021/acs.jctc.6b00343
61. Gritzner, G., Auinger, M.: Statistical analysis of Gibbs energies of transfer of cations and soft solvent parameters. Acta Chim. Slov. **56**(1), 86–94 (2009)
62. Armand, M., Endres, F., MacFarlane, D.R., Ohno, H., Scrosati, B.: Ionic-liquid materials for the electrochemical challenges of the future. Nat. Mater. **8**, 621 (2009). https://doi.org/10.1038/nmat2448
63. Wilkes, J.S.: A short history of ionic liquids—from molten salts to neoteric solvents. Green Chem. **4**(2), 73–80 (2002). https://doi.org/10.1039/B110838G
64. Van Aken, K.L., Beidaghi, M., Gogotsi, Y.: Formulation of ionic-liquid electrolyte to expand the voltage window of supercapacitors. Angew. Chem. Int. Ed. **54**(16), 4806–4809 (2015). https://doi.org/10.1002/anie.201412257
65. Hayes, R., Warr, G.G., Atkin, R.: Structure and nanostructure in ionic liquids. Chem. Rev. **115**(13), 6357–6426 (2015). https://doi.org/10.1021/cr500411q
66. MacFarlane, D.R., Tachikawa, N., Forsyth, M., Pringle, J.M., Howlett, P.C., Elliott, G.D., Davis, J.H., Watanabe, M., Simon, P., Angell, C.A.: Energy applications of ionic liquids. Energy Environ. Sci. **7**(1), 232–250 (2014). https://doi.org/10.1039/C3EE42099J
67. Zhao, Y., Wang, J., Wang, H., Li, Z., Liu, X., Zhang, S.: Is there any preferential interaction of ions of ionic liquids with DMSO and H_2O? A comparative study from MD simulation. J. Phys. Chem. B **119**(22), 6686–6695 (2015). https://doi.org/10.1021/acs.jpcb.5b01925
68. Frisch, M.J., Trucks, G.W., Schlegel, H.B., Scuseria, G.E., Robb, M.A., Cheeseman, J.R., Scalmani, G., Barone, V., Mennucci, B., Petersson, G.A., Nakatsuji, H., Caricato, M., Li, X., Hratchian, H.P., Izmaylov, A.F., Bloino, J., Zheng, G., Sonnenberg, J.L., Hada, M., Ehara, M., Toyota, K., Fukuda, R., Hasegawa, J., Ishida, M., Nakajima, T., Honda, Y., Kitao, O., Nakai, H., Vreven, T., Montgomery Jr., J.A., Peralta, J.E., Ogliaro, F., Bearpark, M.J., Heyd, J., Brothers, E.N., Kudin, K.N., Staroverov, V.N., Kobayashi, R., Normand, J., Raghavachari, K., Rendell, A.P., Burant, J.C., Iyengar, S.S., Tomasi, J., Cossi, M., Rega, N., Millam, N.J., Klene, M., Knox, J.E., Cross, J.B., Bakken, V., Adamo, C., Jaramillo, J., Gomperts, R., Stratmann, R.E., Yazyev, O., Austin, A.J., Cammi, R., Pomelli, C., Ochterski, J.W., Martin, R.L., Morokuma, K., Zakrzewski, V.G., Voth, G.A., Salvador, P., Dannenberg, J.J., Dapprich, S., Daniels, A.D., Farkas, Ö., Foresman, J.B., Ortiz, J.V., Cioslowski, J., Fox, D.J.: Gaussian 09. Gaussian Inc, Wallingford, CT (2009)
69. Becke, A.D.: A new mixing of Hartree–Fock and local density-functional theories. J. Chem. Phys. **98**(2), 1372–1377 (1993). https://doi.org/10.1063/1.464304
70. Lee, C., Yang, W., Parr, R.G.: Development of the Colle–Salvetti correlation-energy formula into a functional of the electron density. Phys. Rev. B **37**(2), 785–789 (1988). https://doi.org/10.1103/PhysRevB.37.785
71. Francl, M.M., Pietro, W.J., Hehre, W.J., Binkley, J.S., Gordon, M.S., DeFrees, D.J., Pople, J.A.: Self-consistent molecular orbital methods. XXIII. A polarization-type basis set for second-row elements. J. Chem. Phys. **77**(7), 3654–3665 (1982). https://doi.org/10.1063/1.444267
72. Hariharan, P.C., Pople, J.A.: Accuracy of AH AnD equilibrium geometries by single determinant molecular orbital theory. Mol. Phys. **27**(1), 209–214 (1974). https://doi.org/10.1080/00268977400100171
73. Hariharan, P.C., Pople, J.A.: The influence of polarization functions on molecular orbital hydrogenation energies. Theor. Chim. Acta **28**(3), 213–222 (1973). https://doi.org/10.1007/bf00533485
74. Hehre, W.J., Ditchfield, R., Pople, J.A.: Self-consistent molecular orbital methods. XII. Further extensions of Gaussian-type basis sets for use in molecular orbital studies of organic molecules. J. Chem. Phys. **56**(5), 2257–2261 (1972). https://doi.org/10.1063/1.1677527
75. Ditchfield, R., Hehre, W.J., Pople, J.A.: Self-consistent molecular-orbital methods. IX. An extended Gaussian-type basis for molecular-orbital studies of organic molecules. J. Chem. Phys. **54**(2), 724–728 (1971). https://doi.org/10.1063/1.1674902
76. Lu, T., Chen, F.: Multiwfn: a multifunctional wavefunction analyzer. J. Comput. Chem. **33**(5), 580–592 (2012). https://doi.org/10.1002/jcc.22885
77. Lu, T., Chen, F.: Quantitative analysis of molecular surface based on improved Marching Tetrahedra algorithm. J. Mol. Graph. Model. **38**, 314–323 (2012). https://doi.org/10.1016/j.jmgm.2012.07.004

78. Dogonadze, R.R., Kalman, E., Kornyshev, A.A.: The Chemical Physics of Solvation: Theory of Solvation. Elsevier, Amsterdam (1985)
79. Fujii, K., Fujimori, T., Takamuku, T., Kanzaki, R., Umebayashi, Y., Ishiguro, S.-I.: Conformational equilibrium of bis(trifluoromethanesulfonyl) imide anion of a room-temperature ionic liquid: Raman spectroscopic study and DFT calculations. J. Phys. Chem. B **110**(16), 8179–8183 (2006). https://doi.org/10.1021/jp0612477
80. Umebayashi, Y., Fujimori, T., Sukizaki, T., Asada, M., Fujii, K., Kanzaki, R., Ishiguro, S.-I.: Evidence of conformational equilibrium of 1-ethyl-3-methylimidazolium in its ionic liquid salts: Raman spectroscopic study and quantum chemical calculations. J. Phys. Chem. A **109**(40), 8976–8982 (2005). https://doi.org/10.1021/jp053476j
81. Singh, D.K., Cha, S., Nam, D., Cheong, H., Joo, S.-W., Kim, D.: Raman spectroscopic study on alkyl chain conformation in 1-butyl-3-methylimidazolium ionic liquids and their aqueous mixtures. ChemPhysChem **17**(19), 3040–3046 (2016). https://doi.org/10.1002/cphc.201600485
82. Xu, A., Zhang, Y., Zhao, Y., Wang, J.: Cellulose dissolution at ambient temperature: role of preferential solvation of cations of ionic liquids by a cosolvent. Carbohydr. Polym. **92**(1), 540–544 (2013). https://doi.org/10.1016/j.carbpol.2012.09.028
83. Zhao, Y., Liu, X., Wang, J., Zhang, S.: Insight into the cosolvent effect of cellulose dissolution in imidazolium-based ionic liquid systems. J. Phys. Chem. B **117**(30), 9042–9049 (2013). https://doi.org/10.1021/jp4038039
84. Gupta, K.M., Jiang, J.: Cellulose dissolution and regeneration in ionic liquids: a computational perspective. Chem. Eng. Sci. **121**, 180–189 (2015). https://doi.org/10.1016/j.ces.2014.07.025